Acta Cryst. (1996). A**52**, 369–378

Anharmonic Motion *vs* Chemical Bonding: on the Interpretation of Electron Densities Determined by X-ray Diffraction

RENZO RESTORI AND DIETER SCHWARZENBACH*

Institute of Crystallography, University of Lausanne, BSP, CH-1015 Lausanne, Switzerland. E-mail: dieter.schwarzenbach@ic.unil.ch

(Received 14 February 1995; accepted 21 November 1995)

Abstract

Anharmonic and electron-density refinements against accurate X-ray diffraction data are today almost routine. However, the unambiguous identification and separation of effects due to anharmonic atomic motion and to chemical bonding is impossible with a single X-ray data set and difficult even with data measured at different temperatures, especially in heavy-atom compounds. For cubic site symmetry, analytical expressions are compared for the convolutions of: (i) the electron density of a spherical free atom with an anharmonic probability density distribution (p.d.f.); and (ii) an aspherical atom with a Gaussian p.d.f. If both the free atom and the deformation functions of the aspherical atom are represented by Gaussian-type functions, there exists for every set of anharmonic parameters an equivalent set of aspherical-atom parameters but the reverse is not necessarily true. Both models are usually suitable for parametrizing anharmonicity also in the case of real atoms and exponential-type deformation functions. Contrary to widespread belief, both models predict a qualitatively similar change of the aspherical density with decreasing temperature: the extrema move towards the atom center and their heights increase except at low temperatures. Quantitatively, however, the temperature dependence of the adjusted parameters should be different: in the case of anharmonicity, the second-, third- and fourth-order coefficients should be proportional to T, T^2 and T^3, respectively, while the population factors of the deformation functions should be independent of T. The theory is tested and verified with refinements on calculated and on measured X-ray structure amplitudes for K_2PtCl_6 at room temperature and at 100 K, and Si at room temperature. Results for K_2PtCl_6 agree well with the anharmonic model. In Si at room temperature, the two effects overlap only slightly and can be reasonably well identified; they cannot be distinguished with simulated high-temperature data.

1. Introduction

X-ray diffraction from a crystalline material provides information on the thermally and spatially averaged electron density in the crystal. If precise measurements are available, the information contained in the structure amplitudes may be interpreted not only in terms of atomic positions and harmonic displacement parameters but also in terms of anharmonic thermal motions and effects due to chemical bonding (Coppens, 1993). The former may be represented by a Gram–Charlier series expansion of a probability density function (Johnson & Levy, 1974), the latter by atom-centered multipolar deformation functions (Stewart, 1976). The parameters of these formalisms are adjusted by least squares to the observed X-ray diffraction data. High correlations between the two types of parameter may be expected if they are adjusted simultaneously, which implies that anharmonicity and bonding effects are not clearly separable.

Features observed in difference-electron-density maps $\delta\rho = \rho - \rho_{pro}$ of organic molecules on or near chemical bonds may safely be attributed to bonding effects; ρ denotes the actual electron density and ρ_{pro} the electron density of the free-atom promolecule model (Hirshfeld, 1991). The interpretation of the difference densities near a heavy atom may be more ambiguous since there $\delta\rho$ may peak sharply at small distances from the atomic center. Near transition-metal atoms in octahedral coordination, for example, $\delta\rho$ has often been observed to show sharp maxima at only 0.3 to 0.4 Å from that atomic center, which point towards the octahedral faces, whereas negative regions are found on the metal–ligand axes (Toriumi & Saito, 1983). Such features have been assumed to represent bonding effects due to the ligand field; the population parameters of the corresponding multipolar functions are then related to the occupancies of the *d* orbitals of the metal atoms (Holladay, Leung & Coppens, 1983). Qualitatively reasonable values of such occupancies have been published, *e.g.* for pyrite-type structures (Stevens & Coppens, 1979; Stevens, DeLucia & Coppens, 1980; Nowack, Schwarzenbach & Hahn, 1991). However, anharmonic motions of the metal atom may result in similar features since they are expected to have larger amplitudes in directions towards second-nearest neighbors and smaller amplitudes towards nearest neighbors. The electron density in K_2PtCl_6 (Restori & Schwarzenbach, 1993) presents another example that is

©1996 International Union of Crystallography
Printed in Great Britain – all rights reserved

at the origin of the present work: it may be parametrized in terms of both anharmonic and multipolar functions since $\delta\rho$ shows compact features close to the atomic centers.

In principle, neutron diffraction should provide an unambiguous identification of anharmonic motions. However, X-ray diffraction from heavy-atom compounds is much more sensitive to anharmonic motions than is neutron diffraction, owing to the very high electron densities at the atom centers and the correspondingly high scattering power at large reciprocal distances. K_2PtCl_6 may serve as an example. The coherent neutron scattering lengths are $b = 9.5$, 3.7 and 9.58 fm for Pt, K and Cl, respectively. The corresponding X-ray values are $(e^2/mc^2)f = 130.5$, 22.2 and 20.6 fm at $\sin\theta/\lambda = 1.0\,\text{Å}^{-1}$ and 52.5, 7.7 and 6.1 fm at $\sin\theta/\lambda = 1.5\,\text{Å}^{-1}$ [*International Tables for X-ray Crystallography* (1974); the symbols e, m, c, f have their usual meanings]. The integrated reflecting power is therefore expected to be at least an order of magnitude larger for X-rays than for neutrons even at very large Bragg angles. So far, we have been unable to measure neutron data for K_2PtCl_6 precisely enough to corroborate or contradict the Gram–Charlier coefficients fitted to an accurate room-temperature X-ray data set.

Alternatively, X-ray experiments carried out at several temperatures should be capable of distinguishing between anharmonic and bonding effects: anharmonic motions are supposed to decrease with temperature but the static electron density obtained by summing the multipolar deformation functions should be independent of temperature. However, in this paper, we show that the variation with temperature of the dynamic thermally smeared density close to heavy atoms is similar for both the anharmonic and the bonding models: the locations and values of the extrema of $\delta\rho$ vary analogously with temperature except at the very lowest temperatures. We will compare these theoretical results with refinements against X-ray data from K_2PtCl_6 and Si.

2. Theory

In the rigid-atom approximation, the dynamic electron density of an atom is described by the convolution product of the static atomic density and a probability density function,

$$\rho_{\text{dyn}}(\mathbf{r}) = \rho_{\text{stat}}(\mathbf{r}) * P(\mathbf{r}). \tag{1}$$

In the anharmonic model (referred to as anh), ρ_{stat} is equal to the free-atom density $\rho_0(r)$ with $r = \|\mathbf{r}\|$ and $P(\mathbf{r})$ is expanded about a Gaussian density function into a Gram–Charlier series. In the bonding-electron-density model (referred to as ED), ρ_{stat} is represented by $\rho_0(r)$ plus a set of multipolar deformation functions and $P(\mathbf{r})$ is a Gaussian density function. In this work, we assume the atom to possess cubic site symmetry; the Gaussian $G(U)$ in the expansion of $P(\mathbf{r})$ is thus isotropic with variance U,

$$G(U) = (2\pi U)^{-3/2}\exp[-(r^2/2U)]. \tag{2}$$

We also assume the free-atom density to be a Gaussian with variance B, $\rho_0(r) = Z\,G(B)$, where Z is the effective atomic number. Typical B values are of the order of $0.01\,\text{Å}^2$ (see below). We choose a unitary coordinate system, *i.e.* coordinate axes of unit length parallel to the cubic lattice base.

The convolution integral for the anharmonically vibrating atom is easily evaluated *via* the Fourier transforms of the Gaussian function and the Gram–Charlier series [Coppens, 1993, equations (1.2.10.3*a*) and (1.2.11.4), respectively]. The Hermite polynomials occurring in the Gram–Charlier expansion of the function $P(\mathbf{r})$ are then decomposed into their multipolar components. Including terms up to fourth order, we obtain for the dynamic atomic electron density $\rho_{\text{anh}}(\mathbf{r})$

$$\begin{aligned}\rho_{\text{anh}}(\mathbf{r}) &= Z\,G(U+B)\{1 + (c^{1111} + 2c^{1122})p_{4,s}(r) \\ &\quad \times [40(U+B)^4]^{-1} + c^{123}p_3(\mathbf{r})/(U+B)^3 \\ &\quad + (c^{1111} - 3c^{1122})p_{4,a}(\mathbf{r})/[60(U+B)^4]\}, \\ p_3 &= x_1x_2x_3, \\ p_{4,s} &= r^4 - 10(U+B)r^2 + 15(U+B)^2, \\ p_{4,a} &= x_1^4 + x_2^4 + x_3^4 - 3x_1^2x_2^2 - 3x_1^2x_3^2 - 3x_2^2x_3^2.\end{aligned} \tag{3}$$

The angular functions p_3/r^3 and $p_{4,a}/r^4$ of the components x_i of $\mathbf{r}$ are proportional to the cubic harmonic functions $K_3 = y_{32-}$ and $K_4 = y_{40+} + y_{44+}/168$, respectively (Kurki-Suonio, 1977), while the polynomial $p_{4,s}$ is spherically symmetric ($l = 0$). An analogous method may be used for calculating ρ_{anh} of an atom with a non-cubic site symmetry, provided $P(\mathbf{r})$ is expanded about an isotropic Gaussian distribution; the Gram–Charlier series then also contains second-order terms.

In the bonding model, the static aspherical atom is represented by

$$\rho_{\text{statED}}(\mathbf{r}) = \rho_0(r) + \sum_{nlm\pm}^{\infty} P_{nlm\pm}L_{lm\pm}y_{lm\pm}\rho_n(r), \tag{4}$$

where $\rho_o(r)$ is represented by a Gaussian function as above, $P_{nlm\pm}$ are population factors, $L_{lm\pm}$ scaling factors and $y_{lm\pm}$ real spherical harmonic functions (Kurki-Suonio, 1977); the radial parts $\rho_n(r)$ are usually expressed as exponential functions $r^n\exp(-\alpha r)$ or, more rarely, with Gaussian functions $r^nG(\sigma)$. We choose a set of functions up to fourth order in l centered on a cubic site which is equivalent to the deformation functions of Hirshfeld (1977): $n = 0$, 2, 4 for $l = 0, n = l$ otherwise. In the case of Gaussian radial functions, the convolution integral (1) for $l \neq 0$ has exactly the same form as for the anh case. With normalizations $L_{lm\pm}$ analogous to Coppens (1993), the

dynamic density $\rho_{ED,G}(\mathbf{r})$ for Gaussian deformation functions becomes

$$\begin{aligned}\rho_{ED,G}(\mathbf{r}) &= Z\,G(U+B) + \rho_{spher}(\mathbf{r}) + G(U+\sigma)\\ &\times \{P_{K3}(\pi\sigma)^{3/2}p_3(\mathbf{r})/(U+\sigma)^3\\ &+ P_{K4}(32\sigma^2/45\times 3^{1/2})p_{4,a}(\mathbf{r})/(U+\sigma)^4\},\\ \rho_{spher}(r) &= G(U+\sigma)\{[P_{000}+P_{200}U/(U+\sigma)\\ &+ P_{400}U^2/(U+\sigma)^2] + [P_{200}\sigma/(U+\sigma)^2\\ &+ 2P_{400}U\sigma/(U+\sigma)^3]r^2/3\\ &+ [P_{400}\sigma^2/(U+\sigma)^4]r^4/15\}.\end{aligned} \tag{5}$$

The first term is the spherical density of the thermally smeared free atom as in (3); $\rho_{spher}(r)$ is a function of the monopolar population factors P_{n00} as well as of U and σ and represents the spherically symmetric deformation density; P_{K3} and P_{K4} are the populations of the cubic multipoles of order $l = 3$ and 4, respectively ($n = l$); p_3 and $P_{4,a}$ are defined in (3).

The comparison of (3) and (5) shows that the dynamic atomic densities of the two models are described by the same type of function: for every set of values B, U_{anh} and c^{jkmn} in (3), there exists an equivalent set σ, U_{ED} and $P_{nlm\pm}$ in (5):

$$\begin{aligned}\sigma &= B, \quad U_{ED} = U_{anh},\\ P_{000} &= (3/8)Z(c^{1111}+2c^{1122})/B^2,\\ P_{200} &= -2P_{000}, \quad P_{400} = P_{000},\\ P_{K3} &= Zc^{123}/(\pi B)^{3/2},\\ P_{K4} &= (3\times 3^{1/2}/128)Z(c^{1111}-3c^{1122})/B^2.\end{aligned} \tag{6}$$

Thus, for each successful parametrization of a data set in terms of the anh model, there exists a completely equivalent parametrization in terms of the Gaussian ED model, provided that the approximation of the free-atom density by a Gaussian is satisfactory. The converse is of course not true since σ, U_{ED} and all $P_{nlm\pm}$ are independently adjustable. The ED model is the more flexible because the anharmonicity affects all electrons while bonding affects mainly the valence shell. Correspondingly, B is a property of the free atom, in contrast to σ. However, if the numerical values of B and σ are similar, the ED model efficiently parametrizes anharmonic effects.

The extrema of the lth-order multipolar terms of (3) occur at distances r_{extr} from the atomic center,

$$\begin{aligned}r_{extr}(l\neq 0) &= [l(U+B)]^{1/2},\\ r_{extr}(l=0) &= \{[7\pm(14)^{1/2}](U+B)\}^{1/2} \quad \text{and} \quad 0;\end{aligned} \tag{7}$$

$l = 0$, 3 and 4 refer to the $p_{4,s}$, p_3 and $p_{4,a}$ polynomials, respectively. The values of the extrema are proportional to $(U+B)^{-(l+3)/2}$. At or above room temperature, U usually dominates over B. We conclude that the shape of the dynamic electron densities in both the anh and the ED models (where B is replaced by σ) show qualitatively the same dependence on the temperature. The extrema move towards the atom center with decreasing temperature. The values of the extrema are commonly believed to behave differently for the two models since the c^{jkmn} should tend to zero and $P_{nlm\pm}$ should remain constant. However, for $U > B$, the values of the extrema are expected to increase with decreasing temperature even in the anharmonic case since the decrease of c^{jkmn} is more than balanced by the increase of $(U+B)^{-(l+3)/2}$. Only towards very low temperatures is the evolution of the densities of the two models expected to be very different.

In electron-density refinements, exponential-type radial functions $r^n\exp(-\alpha r)$ are more widely used than Gaussian-type functions. The far more complicated evaluation of the convolution integral (1) for exponential functions to obtain $\rho_{ED,E}(\mathbf{r})$ is given in Appendix A. Relevant results are similar to those derived from (5). Using again the normalizations of Coppens (1993), we get

$$\begin{aligned}\rho_{ED,E}(\mathbf{r}) &= Z\,G(U+B) + P_{000}g_{00}/8\pi + P_{200}g_{20}/96\pi\\ &+ P_{400}g_{40}/2880\pi + P_{K3}[p_3(\mathbf{r})/r^3]g_{33}/60\\ &+ P_{K4}[p_{4,a}(\mathbf{r})/r^4]g_{44}/(270\times 3^{1/2}\pi),\end{aligned} \tag{8}$$

where the functions $g_{nl}(r,\alpha,U)$ given in Appendix A replace the Gaussian-type functions $r^nG(U+\sigma)$ in (5) or $r^nG(U+B)$ in (3). The distances of the extrema of the g_{nl} from the atomic center can be calculated numerically. For any given values of U and B (or σ), there exists a value for α such that these distances are the same for both formalisms. Numerical calculations for $n = l$ show that $\alpha(U,B)$ generally increases with increasing values of U and decreasing values of B and is somewhat larger for $n = 4$ than for $n = 3$; it depends only weakly on U for $U > 0.02$ Å^2. Typical values of α for B in the range 0.005 to 0.02 Å^2 are 40 to 15 Å^{-1}. Most importantly, for $U > B$ (or σ), the Gaussian-type function is an excellent approximation of g_{nl}. Fig. 1 shows that, for $l \neq 0$, it is still a moderately good approximation for U as small as

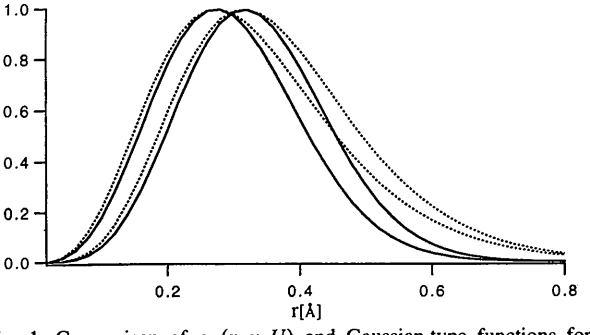

Fig. 1. Comparison of $g_{nl}(r,\alpha,U)$ and Gaussian-type functions for $l = n = 3$ and 4. Solid lines are proportional to $r^nG(U+B)$ with $U = 0.005$ Å^2, $B = 0.02$ Å^2; dotted lines are proportional to g_{nn} with $\alpha_3 = 14.4$ Å^{-1}, $\alpha_4 = 16.4$ Å^{-1}.

$B/4$. Fig. 2 shows a close fit of a combination of g_{n0} functions with the spherical part of (3) even for small U. The overall shape of g_{nl} depends only weakly on α; therefore, linear combinations of g_{nl} with a common value of α can in general be fitted reasonably well to corresponding linear combinations of Gaussian-type functions with a common value of σ or B.

We conclude that ED refinements with Gaussian and exponential functions should give very similar results and that $\rho_{\rm anh}(\mathbf{r})$ may also be parametrized successfully with exponential deformation functions, except at very low temperatures. The most questionable approximation in the theory is the representation of the free-atom density $\rho_0(r)$ by a Gaussian function $ZG(B)$ [(2)]. The Gaussian decreases much faster with r than the actual ρ_0. Thus, the effective Z for the best fit of the two functions is usually much smaller than the number of electrons of the atom, *e.g.* $Z \simeq 8$ e, $B \simeq 0.01$ Å^2 for K. For real atoms, the agreements with the observed diffraction data obtained from the anh, (ED, G) and (ED, E) models will therefore not be exactly identical. In addition, the refined value of U is expected to be model dependent. In what follows, we discuss refinements of the structures of K_2PtCl_6 and Si and their interpretations in terms of anharmonic motion and bonding effects.

3. Electron density of K_2PtCl_6

Commercially available K_2PtCl_6 powder (Fluka puris. p.a., 40 wt% of Pt) was recrystallized from distilled water. The chemical composition was ascertained by electron probe microanalysis (instrument ARL-SEMQ) of five crystals from the same batch as the one used for the diffraction experiments. The reference standards were KCl (puris. Fluka, >99.5%) and metallic Pt. All crystals were covered by a layer of gold 300 Å thick to ensure the necessary electrical and thermal conductivities. The cross section of the electron beam was 50×50 μm. The characteristic emissions analyzed were $K\alpha$ of K and Cl, and $M\alpha$ of Pt. After the usual corrections for absorption and secondary fluorescence, averaged results of the analyses are 16.74 (14), 38.26 (67) and 45.00 (71) wt% for K, Pt, and Cl, respectively. The e.s.d.'s represent the sample variances. The respective calculated values for pure K_2PtCl_6 are 16.09, 40.14 and 43.77 wt%. The underestimation of Pt with respect to K and Cl is probably due to systematic errors since different reference standards with strongly differing thermal and electrical properties had to be used. The atomic ratio of Cl to K, determined with a single reference standard, is 2.96 (5). We conclude that impurities, *e.g.* NH_4^+ replacing K^+, amount to less than 1 at.%.

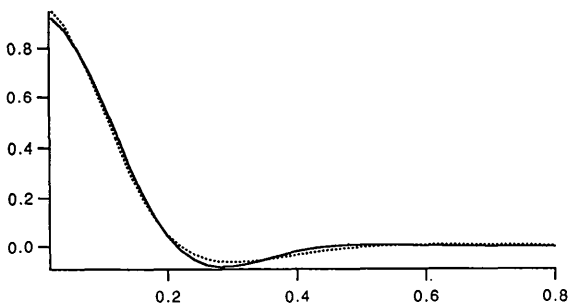

Fig. 2. Comparison of spherically symmetric $g_{n0}(r, \alpha, U)$ and Gaussian-type functions. Solid line proportional to $p_{4,s}G(U+B)$ of (3) with $U = 0.005$ Å^2, $B = 0.02$ Å^2; dotted line $K_0g_{00} + K_2g_{20} + K_4g_{40}$ with $\alpha = 12.8$ Å^{-1}. The K_n have been adjusted to produce a close fit of the curves.

K_2PtCl_6 crystallizes in the cubic space group $Fm\bar{3}m$, $Z = 4$, $a = 9.743$ (3) Å at room temperature. Site symmetries are $m\bar{3}m$ for Pt at 0, 0, 0; $\bar{4}3m$ for K at 1/4, 1/4, 1/4 and $4mm$ for Cl at $x, 0, 0$ ($x \simeq 0.237$). Refinements of various combinations of anh and ED models were reported by Restori & Schwarzenbach (1993, hereafter referred to as RS). At room temperature, three of these models provided satisfactory parametrizations of the densities near K and Cl: (i) Gram–Charlier formalism; (ii) exponential-type electron-density functions with two exponents α for each atom, one for the monopolar and another for the multipolar terms; (iii) both anharmonic and electron-density functions with a single exponent per atom. Model (i) provided the most economical parametrization but this is *per se* not sufficient to prove the presence of anharmonic motions. The corresponding difference electron-density maps (Restori & Schwarzenbach, 1993, 1995) show a prominent octopolar density centered on K with maxima of ~0.5 e Å^{-3} peaking on the tetrahedral ⟨111⟩ directions at ~0.4 Å from the atom center. Several (unpublished) neutron data sets were not sufficiently accurate to corroborate the anharmonic interpretation. The room-temperature X-ray data set containing 489 absorption-corrected inequivalent intensities measured with Ag $K\alpha$ radiation ($\lambda = 0.5608$ Å) to $(\sin\theta/\lambda)_{\rm max} = 1.3$ Å^{-1} has been deposited by Restori & Schwarzenbach (1995). In this paper, we report anh and ED refinements against simulated data, against the room temperature data of RS and against an additional data set measured at 100 K using the same crystal as RS* (Table 1). Atomic form factors and the dispersion corrections for Ag radiation were taken from *International Tables for X-ray Crystallography* (1974). We concentrate mainly on the site of K. Cl has nearly the same diffracting power but is described by many more parameters. We also report aspherical densities near Pt. The significance of the spherical anharmonic terms is doubtful, the free-atom form factors and dispersion factors, in particular those of Pt, being of uncertain quality.

* Structure amplitudes at 100 K have been deposited with the IUCr (Reference: CR0500). Copies may be obtained through The Managing Editor, International Union of Crystallography, 5 Abbey Square, Chester CH1 2HU, England.

Table 1. *Data collection of K_2PtCl_6 at 100 K*

Crystal data

$M_r = 486.012$	Cell parameters for 16 reflections
$a = 9.673$ (2) Å	$\theta = 7$–$14.5°$
$V = 905.1$ (6) Å^3	$\mu = 9.76$ mm^{-1}
$D_x = 3.567$ Mg m^{-3}	$T = 100$ (2) K
Ag $K\alpha$ radiation	Octahedron {111}
$\lambda = 0.5608$ Å	0.097 (2) mm between faces

Data collection and refinement

Enraf–Nonius CAD-4 diffractometer	$h, k, l = 0, 0, 0 \rightarrow 30, 30, 30$
$\omega/2\theta$ scans	3 standard reflections monitored every 2 hours
Absorption correction: analytical	intensity variation insignificant
$T_{min} = 0.452$, $T_{max} = 0.496$	Refinements on $\|F\|^2$
10941 measured reflections	Weights $w = 1/\sigma(\|F\|^2)$
758 independent reflections	Extinction correction:
758 observed reflections	Becker & Coppens (1974, 1975)
$[I > 10\sigma(I)]$	type I, Lorentzian distribution
$R_{int} = 0.017$	
$\theta_{max} = 60°$	

3.1. *Refinements against calculated intensities*

The theoretical results were first tested with ED least-squares refinements using exponential functions. $|F_c|^2$ values calculated with the anh model for K served as observations; they were not modified with random errors. Weights were chosen proportional to $|F_c|^{-2}$ so as to be roughly similar to the weights of the measured diffraction data. Each of the resulting data sets of simulated intensities comprised 1126 reflections with $(\sin\theta/\lambda)_{max} = 1.76$ Å^{-1}. First, structure amplitudes were calculated with harmonic displacement parameters for all atoms and a single anharmonic term for K, either third order with the numerical value from a refinement of the 293 K data (Table 2) or fourth-order aspherical or fourth-order spherical. Corresponding refined α values of the ED model will be denoted by α_3, $\alpha_{4,a}$ and $\alpha_{4,s}$. Subsequently, larger anharmonic terms and/or smaller values of U(K) down to 0.005 Å^2 were assumed. Finally, all three anharmonic terms of K were included together.

For data including only the small c^{123}(K) term from Table 2, a standard refinement including only harmonic displacement factors gave $R(|F|) = 0.00128$. Note that c^{123} does not contribute to the reflections with parity *eee*. The largest discrepancies between simulated and calculated structure factors of about 0.65 e (about 1% of $|F|$) occurred in the $\sin\theta/\lambda$ range of 0.6 to 0.8 Å^{-1}. When the population of an ED octopole is refined, $R(|F|) = 0.00004$ and $\alpha(\text{K}) = 33\,(2)$ Å^{-1}. This shows that the anharmonic motion as observed in refinement *A* of RS can be modeled nearly perfectly with an exponential-type electron-density function. When c^{123}(K) is ten times larger, $R(|F|)$ also increases tenfold but is still very small.

Assuming different values for U(K) shows that $R(|F|)$ increases with decreasing values of U(K). The characteristics of α(K) are: $\alpha_{4,a}$ is about 10% larger than α_3; all α(K) increase with decreasing U(K); for data including a single anharmonic term, refined values of α(K) depend on U(K) and also on the e.s.d.'s assigned to the simulated intensities. For data computed with the aspherical anharmonic terms, refined values of U(K) are similar to the values used for generating that data. In contrast, for data computed with the spherical anharmonic term and $U(\text{K}) < 0.04$ Å^2, refined values of U(K) and $\alpha_{4,s}$(K) are strongly correlated. In this case, the refined value of U(K) is biased: if $c^{1111} + 2c^{1122} > 0$, it is smaller than the value used for generating the data and *vice versa*. Corresponding reliability factors are small even for small values of U(K). Refinements on data sets including all anharmonic terms of K confirm these results, except that the refined value of α(K) depends on the relative magnitudes of the terms as much as on the value of U(K).

Refinements on data generated with all anharmonic terms of K of Table 2 and $U(\text{K}) = 0.005$ Å^2 never result in $R(|F|) > 0.001$. X-ray data measured at 8 K (unpublished) indicate that $U(\text{K}) > 0.005$ Å^2 at the lowest temperatures. Therefore, the anh and the ED model are both capable of producing an acceptable fit to the data of K_2PtCl_6 at all temperatures, in agreement with theory.

3.2. *Deriving the variance B of the Gaussian atom from real data*

The parameter B of (3) may be estimated from the results of anharmonic refinements on the room-temperature and 100 K data (Table 2). Maps of partial dynamic density were drawn for each contributing term separately by summing Fourier series of partial structure factors. From (7), the positions of the extrema give four independent estimates of $U + B$, two for $l = 0$ and one each for $l = 3$ and 4. The extremum for the + sign of $l = 0$ is weak and difficult to localize. This leaves three estimates at each temperature (Table 3). Additional estimates for $U + B$ obtained from the extremal values of the densities are less accurate because of series-termination errors, particular at 100 K. The precision is also limited by the finiteness of the grid. With the values for U(K) taken from Table 2, B(K) is 0.0068 (10) Å^2 at 293 K and 0.0099 (8) Å^2 at 100 K. These results are in fair agreement with the value of 0.0102 Å^2 obtained by fitting a Gaussian to the Fourier transform of the form factor of K. Thus, the locations of the maxima of electron density are reasonably consistent with the approximation of the free-atom density by a Gaussian.

3.3. *Refinements against real data*

In these refinements, the parameters of all atoms, K, Cl and Pt, were adjusted. Refinements were terminated if all ratios (full shift/standard deviation) $< 10^{-4}$. Reliability factors, displacement parameters U, difference density and residual maps at 293 K obtained for the anh, ED and combined anh–ED models have been published in RS. In

Table 2. *Results of the anharmonic and standard harmonic (*) refinements of K_2PtCl_6*

The anharmonic coefficients c^{jkmn} are multiplied by 10^4, the dimension of the nth order is $Å^n$ (coordinate system with axial lengths 1).

	293 K	100 K
S	1.213	1.514
	2.080*	1.828*
$R(\|F\|)$	0.0067	0.0064
	0.0119*	0.0076*
$wR(\|F\|^2)$	0.0091	0.0112
	0.0157*	0.0136*
K		
U (Å^2)	0.03784 (15)	0.01343 (5)
	0.03697 (7)*	0.01286 (2)*
c^{123}	4.2 (4)	0.46 (8)
c^{1111}	0.9 (2)	0.37 (5)
c^{1122}	0.27 (14)	0.10 (2)
Pt		
U (Å^2)	0.01559 (3)	0.00494 (2)
	0.01465 (1)*	0.004601 (4)*
c^{1111}	0.60 (3)	0.120 (6)
c^{1122}	0.27 (1)	0.043 (2)

	293 K	100 K
Scale	2.983 (2)	1.2381 (7)
	2.944 (1)*	1.2252 (4)*
10^4 g_{ext}	0.321 (2)	0.116 (3)
	0.286 (2)*	0.080 (3)*
Cl		
x	0.23719 (3)	0.23920 (2)
	0.23743 (2)*	0.23926 (1)*
U_{11} (Å^2)	0.01665 (12)	0.00628 (5)
	0.01606 (6)*	0.00581 (2)*
U_{22} (Å^2)	0.04342 (16)	0.01642 (6)
	0.04168 (7)*	0.01570 (2)*
c^{111}	0.0 (2)	0.09 (9)
c^{122}	−2.7 (5)	−0.33 (7)
c^{1111}	0.14 (14)	0.20 (4)
c^{2222}	2.9 (4)	0.55 (5)
c^{1122}	0.49 (8)	0.134 (13)
c^{2233}	0.5 (2)	0.09 (3)

order to reveal the aspherical features in these maps, the spherical features centered on the atoms were fitted with empirically chosen functions and then subtracted. This procedure failed when applied to the corresponding maps obtained at 100 K: there, the series-termination effects are much more pronounced than at room temperature and significant features are immersed in noise arising from ripples about the atomic centers. An extension of the Fourier series with calculated high-order data is not practical because $(\sin\theta/\lambda)_{max} > 3$ Å^{-1} would be required to reduce the intensity of the ripples to the (non-negligible) level observed at room temperature. Therefore, we do not present any maps at 100 K and discuss only the fits obtained in the refinements.

Refinement A: The refinements of the parameters of the anh model (*A* of RS) result in acceptable agreements with the observations at both 293 and 100 K (Table 2). The displacement factors U are larger than those obtained with standard harmonic refinements by 2 to 8%, on average by 3.6% at 293 K and 5.1% at 100 K. The residual maps show no significant features near K and Cl (see RS). Results at the two temperatures are qualitatively very similar and differ only in some details: (i) the dominating third-order terms of both K and Cl have the same signs and contribute similarly to ρ_{anh} of (3); (ii) the values of the extrema of the third-order term of K are proportional to $c^{123}(U+B)^{-3} = 4.6\,(5)$ Å^{-3} at 293 K and 3.4 (7) Å^{-3} at 100 K and thus are similar. The fourth-order terms, however, are relatively more important at 100 K.

Refinement B: The ED model equivalent to the Hirshfeld model with a single radial exponent α per atom, as described in §2, was relatively unsuccessful at room temperature [refinement *B* of RS, $S = 1.334$, $wR(|F|^2) = 0.00986$, $\alpha(\mathrm{K}) = 7.2\,(5)$ Å^{-1}, $U(\mathrm{K}) = 0.0350\,(3)$ Å^2]: reliability factors are higher than for the anh model *A*; the residual map in RS shows that a large portion of the features about K and Cl is not accounted for; α(K) is much smaller than the expected value of about 33 Å^{-1}. This contrasts with the theoretical predictions and the refinements on calculated data. In fact, the least-squares minimum published in RS is not unique. Starting the refinement with $\alpha(\mathrm{K}) = 35$ Å^{-1} leads to an apparently different minimum at $wR(|F|^2) = 0.00982$, $\alpha(\mathrm{K}) = 19\,(3)$ Å^{-1} and $U(\mathrm{K}) = 0.0207\,(45)$ Å^2 but the density around K is still not fully parametrized as evidenced by a residual map showing important features. The value of U(K) is unrealistically small, its large e.s.d. being due to an important correlation with α(K). When U(K) is fixed at 0.0378 Å^2 as obtained in the anh model, the refinement converges at $wR(|F|^2) = 0.00991$ and $\alpha(\mathrm{K}) = 24\,(3)$ Å^{-1}; the corresponding residual map in the region of K is flatter than before but still not acceptably flat. We conclude that the standard ED model does not result in a unique parametrization of the 293 K data and always appears to be less successful than the anh model. For the 100 K data, the least-squares minimum was found at $S = 1.248$, $wR(|F|^2) = 0.00918$, $\alpha(\mathrm{K}) = 27\,(6)$ Å^{-1} and $U(\mathrm{K}) = 0.0158\,(25)$ Å^2, *i.e.* at lower reliability factors than for refinement *A* but an unacceptably large value for U(K).

Table 3. *Estimates of $U + B$ (Å^2) of thermally smeared K, derived from the extrema of partial electron densities of order l along direction [uvw] using (7)*

l	[uvw]	293 K	100 K
3	[111]	0.0449 (10)	0.0238 (8)
4, s	Spherical	0.0443 (10)	0.0222 (7)
4, a	[100], [111]	0.0447 (10)	0.0241 (7)

Refinements C and D: In RS, it was shown that an ED model including more functions ($l = 3$, $n = 5$; $l = 4$, $n = 6$) was as unsuccessful as model *B* in parametrizing the densities near K and Cl as long as one single radial exponent α per atom was used (refinement *C*). In contrast, the adjustment of two radial exponents, α_{spher} for the monopolar functions and α_{aspher} for the aspherical functions, resulted in a flat residual density (refinement *D* of RS). At both temperatures, $\alpha_{spher}(K) \simeq 4 \text{Å}^{-1}$ and $\alpha_{spher}(K) \simeq 24$ to 30Å^{-1}, but convergence was difficult to attain because of high correlations between the parameters.

3.4. *Arguments in favor of anharmonicity*

We conclude that the anh model parametrizes the electron densities at K and Cl efficiently at both temperatures. The basic ED model is clearly inferior at room temperature, even though it comprises more adjustable parameters; but at 100 K, judging only from the reliability factors, it appears to be at least as suitable as the anh model. Remembering that both models are parametrization schemes rather than physical theories, arguments in favor of the one or the other must be based on consistency with physical or chemical theories instead of on the fit with the diffraction data. The most obvious property to investigate is the temperature dependence of the refined quantities. The ED populations $P_{nlm\pm}$ ought to be independent of the temperature whereas the displacement factors depend on the temperature: $U \simeq k_2 T$ above the Debye temperature, $c^{jkm} \simeq k_3 T^2$, $c^{jkmn} \simeq k_4 T^3$, where k_2, k_3, k_4 are proportionality constants (Willis & Pryor, 1975). If the ED model has been used to represent anharmonicity instead of bonding effects, then the ED populations are functions of temperature as evidenced by (6).

Fig. 3 shows that the temperature dependence of the *U*'s and the c^{jkm} agrees reasonably well with the predictions of the anh model. At 100 K, the *U*'s are somewhat larger than predicted by a straight line passing through the origin, except for Pt, as would be expected for a temperature near the Debye temperature. The Pt—Cl bond is nearly, but not quite, rigid since $U_{11}(Cl) > U(Pt)$. $U_{22}(Cl)$ and $U(K)$ are of the same order of magnitude; we recall that K and Cl together form a cubic close packing. The aspherical fourth-order term $c^{1111} - 3c^{1122}$ of K is negligibly small; that of Pt agrees very closely with the T^3 law (not shown in the figure). The spherical fourth-order terms $c^{1111} + 2c^{1122}$ of K and Pt, however, decrease relatively slowly with only $T^{0.9}$ and $T^{1.6}$, respectively. Their physical significance is not clear. They may in part be due to bonding features but monopolar quantities are also most sensitive to deficiencies of the model, such as uncertainties in the free-atom scattering factors and the extinction correction. The fourth-order c^{jkmn} of Cl cannot be decomposed easily into aspherical and spherical contributions since the harmonic *U*'s are distinctly anisotropic; individually, they do not obey the T^3 law.

In contrast, the populations obtained with the ED refinement for the two temperatures differ strongly. We also recall that refinements *B* result in *U* values that differ considerably from those obtained in refinements *A* and the standard harmonic refinements. Since the dominant third-order aspherical electron-density features near K and Cl obey the T^2 law, we conclude that anharmonic effects are much more important than bonding effects. The geometric interpretation of the former is obvious: the amplitude of the vibration of K is larger towards the unoccupied octahedral void in the packing of Cl and smaller towards the void occupied by Pt; the c^{122}(Cl) coefficient agrees with the curvilinear movement of Cl on the surface of a sphere corresponding to the libration of the $PtCl_6$ octahedron. Pt also appears to exhibit a small anharmonic motion; the sign of $c^{1111} - 3c^{1122}$ indicates larger displacements towards the faces of the coordination octahedron.

Hester, Maslen, Spadaccini, Ishizawa & Satow (1993) have published a very different interpretation of $\delta\rho$ maps for K_2SiF_6 whose structure is isomorphous with K_2PtCl_6. The difference density near K is very similar in both structures. The authors argue against anharmonicity and in favor of bonding effects because they find qualitatively similar features at 100 K and at room temperature.

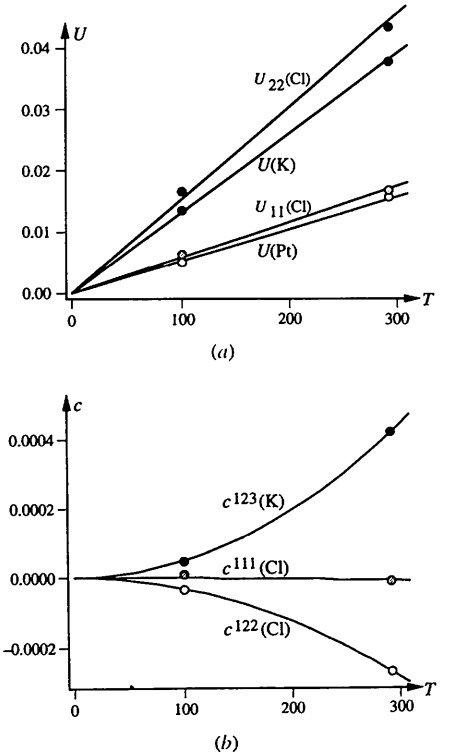

Fig. 3. Plots of (*a*) the harmonic and (*b*) the third-order anharmonic displacement parameters in K_2PtCl_6 *vs* temperature *T*; anharmonic refinement *A*.

The present work shows that this result agrees with both anharmonic and bonding effects and that the argument in favor of the latter is not conclusive.*

4. Anharmonicity in silicon

Silicon is known to exhibit anharmonicity in addition to electron-density effects even at room temperature (Roberto, Batterman & Keating, 1974). Precise structure amplitudes measured with the *Pendellösung* method have been reported by Teworte & Bonse (1984) and by Saka & Kato (1986). These data have been used extensively in recent years to study the electron density (Spackman, 1986) and to test maximum-entropy methods (Sakata & Sato, 1990; Jauch & Palmer, 1993). They include 61 structure amplitudes, 30 measured at $\lambda = 0.4$ Å, 16 with Ag $K\alpha_1$ and 15 with Mo $K\alpha_1$ radiation; they do not include any pseudo-extinct reflections with parity $h+k+l = 4n+2$; $(\sin\theta/\lambda)_{max} = 1.04$ Å^{-1}; $a = 5.431$ Å. We have used these data to ascertain the presence of anharmonic motion and to test the separability of anharmonic and bonding effects. Consequently, we have refined two models (Table 4):

(*A*) the ED model given by (4) and (8) with exponential radial functions, comprising as adjustable parameters U, P_{000}, P_{200}, P_{400}, P_{K3}, P_{K4} and α;

(*B*) the combined ED and anh model, comprising the parameters of (*A*) and c^{123}, c^{1111} and c^{1122}.

Atomic form factors and the dispersion corrections for Mo and Ag radiation were taken from *International Tables for X-ray Crystallography* (1974). The dispersion corrections for $\lambda = 0.4$ Å were estimated to be $f' = 0.017$ and $f'' = 0.018$ e. The results do not depend sensitively on these values; an increase of all f' by 10% in model *B* affects the value of U by 2.6 e.s.d.'s and the other parameters by only a few tenths of an e.s.d.

The values of U obtained in refinements *A* and *B* (Table 4) agree well with the value of 0.00579 (1) Å^2 reported by Saka & Kato (1986). The third-order anharmonic coefficient in model *B* is in close agreement with the value of $17.8\,(18) \times 10^{-6}$ Å^3 calculated using U and the structure factor of the 222 reflection from neutron diffraction at 288 K (Roberto, Batterman & Keating, 1974). The anharmonic fourth-order terms have been ignored in previous work; in the present refinements, the spherical component in particular appears to be non-

Table 4. *Results of the refinements of Si*

The anharmonic coefficients c^{jkmn} of model *B* are multiplied by 10^6, the dimension of the *n*th order is Å^n (coordinate system with axial lengths 1).

	Model *A*	Model *B*
S	4.446	3.554
$R(\|F\|)$	0.00113	0.00120
$wR(\|F\|^2)$	0.00158	0.00123
U (Å^2)	0.005817 (2)	0.005754 (6)
P_{000}	−0.31 (3)	−0.26 (3)
P_{200}	−3.4 (3)	−2.5 (3)
P_{400}	3.7 (3)	2.8 (3)
P_{K3}	−1.89 (9)	−1.64 (8)
P_{K4}	−0.85 (5)	−0.71 (5)
α	3.00 (4)	3.11 (4)
c^{123}		19.7 (19)
c^{1111}		−7.3 (8)
c^{1122}		−3.8 (3)

negligible. The dynamic density due to the anharmonic terms shows extrema of +0.8 and −1.4 e Å^{-3} at a distance of 0.18 Å from the center of the atom (Fig. 4). The dominating third-order term contributes ±1.1 e Å^{-3}. For comparison, the dynamic difference density centered in the middle of the Si—Si bond amounts to only 0.2 e Å^{-3}. Even though the ED populations and α values, and therefore the static bonding densities, from refinements *A* and *B* differ slightly, the corresponding dynamic densities (calculated with the ED deformation functions only) are indistinguishable. We conclude that the effects of anharmonicity and bonding overlap slightly even though the respective features appear to be well separated.

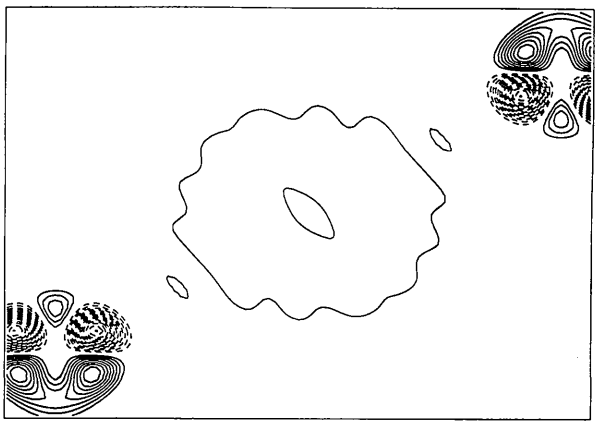

Fig. 4. Dynamic difference density $\delta\rho = \rho - \rho_{pro}$ in silicon, plane $(1\bar{1}0)$, [111] from lower left to upper right, obtained with a Fourier summation of structure factors calculated with the anharmonic and electron-density coefficients of refinement *B*; $(\sin\theta/\lambda)_{max} = 1.6$ Å^{-1}. Contour intervals are 0.1 e Å^{-3}, the zero contour is omitted. The Si—Si distance separating the centers of the octopoles is 2.352 Å. The wiggles of the 0.1 e Å^{-3} contour about the midpoint of the Si—Si bond are due to series-termination effects; they are absent if the structure factors are calculated with the deformation functions only.

* One of the referees remarked that K_2PtCl_6 is easily contaminated by NH_4^+ replacing K^+. Electron probe microanalysis indicates this contamination to be less than 1% of K^+. NH_4^+ forms hydrogen bonds with the 12 neighboring Cl atoms and is therefore orientationally disordered. The contribution to $\delta\rho$ of a disordered H atom of an impurity constituent is expected to be minor. The observed extrema near K are not located on K–Cl contacts, their value of 0.5 e Å^{-3} approaches that expected for an ordered H atom near 100% occupancy and their distance of 0.4 Å from the atom center is far too short for an N—H bond.

Which properties may be determined at high temperature? To answer this question, we have calculated diffraction data with the following parameters: U and c[123] 6 times and 36 times larger, respectively, than the values found at room temperature, corresponding to a temperature of about 2500 K, the Debye temperature being 543 K; population parameters of the deformation functions of refinement B; no fourth-order anharmonic terms; $(\sin\theta/\lambda)_{max} = 1.6\,\text{Å}^{-1}$; $\sigma(|F|^2) = 2|F|$. The corresponding dynamic difference density map resembles closely that of K_2PtCl_6 near K (see RS): extrema of height $\pm 0.72\,\text{e Å}^{-3}$ are found at a distance of 0.36 Å from the center of the atom. Note that the value of these extrema is smaller than at room temperature. The parameters of model A were then refined against these synthetic data to $R|F| = 0.008$. This shows that the ED functions are perfectly capable of representing the anharmonic motion of Si but they do not parametrize at all the comparatively weak bonding effects in the middle of the Si—Si bond. With the high-temperature data alone, it would be impossible to distinguish between anharmonicity and bonding.

5. Conclusions

The bonding-electron-density and anharmonic models are often used as parametrization schemes rather than as physical theories. A successful refinement of a model as judged by the quality of the fit with the experimental data yields a picture of the thermally smeared electron density but usually it does not provide a physical interpretation of the result. Even though the anh and ED models, when applied to real data do not give exactly the same results, both are usually capable of giving satisfactory agreement factors. The interpretation of electron-density maps is therefore ambiguous, in particular in the case of heavy-atom compounds.

The conventional view that anharmonicity and bonding effects can be distinguished with X-ray data measured at different temperatures is essentially correct. Contrary to widespread belief, however, this cannot be achieved by visual inspection of dynamic difference density maps since the relevant features vary in qualitatively the same way with temperature for both models: the lower the temperature, the closer to the atom center are the extrema of the difference density while the values of the extrema increase or are roughly constant. Arguments for the correct model are given by the temperature dependence of harmonic and anharmonic displacement factors, and of population factors of deformation functions: the former should vary with T, T^2 and T^3 according their order and symmetry, the latter should be independent of temperature. However, the anharmonic terms of atoms on non-cubic sites are not easily decomposed into their multipolar components if the Gram–Charlier series is developed about an anisotropic Gaussian. Fourth-order coefficients representing a combination of monopolar, quadrupolar and hexadecapolar properties are not expected to vary with a simple T^3 law.

A joint refinement of anh and ED parameters may give meaningful results only if the corresponding electron-density features are well separated in space, some being found near the atomic centers and others in the internuclear region. However, an alternative pure ED model comprising two sets of functions with very different values of the exponents α should then also be successful. A satisfactory analysis of an electron density comprising important contributions of both anharmonicity and chemical bonding to the same region of space is well nigh impossible with X-ray data alone.

The aspherical density features in K_2PtCl_6 are all found near the atom centers. They appear to be due nearly exclusively to anharmonicity as evidenced by the excellent fit of the T^2 and T^3 laws with the aspherical anharmonic displacement factors of all atoms. In Si at room temperature, anharmonicity and bonding features occupy very different regions in space and their contributions can therefore be identified with a certain degree of confidence.

We thank Mr G. Burri for carrying out the electron probe microanalysis of K_2PtCl_6. This work has been supported by the Swiss National Science Foundation.

APPENDIX A

The convolution of an exponential-type deformation electron-density function (with normalizing factors) and a Gaussian function is the integral

$$\begin{aligned}\rho_{nlm\pm} &= [(2\pi U)^{-3/2}\exp(-r^2/2U)] \\ &\quad * [\alpha^{3+n} r^n y_{lm\pm}\exp(-\alpha r)] \\ &= \alpha^{n+3}(2\pi U)^{-3/2}\int_0^\infty u^{n+2}\exp(-\alpha u)\,du \\ &\quad \times \int_\Omega \exp(-|\mathbf{r}-\mathbf{u}|^2/2U)\,y_{lm\pm}\,d\Omega,\end{aligned}$$

where $y_{lm\pm}$ is an angular surface harmonic function. Expansion of $|\mathbf{r}-\mathbf{u}|^2 = r^2 + u^2 - 2\mathbf{r}\cdot\mathbf{u}$ leads to the integral

$$\int_\Omega \exp(\mathbf{u}\cdot\mathbf{r})\,y_{lm\pm}(\theta_2,\varphi_2)\,d\Omega_2 = 4\pi i_l(ur)\,y_{lm\pm}(\theta_1,\varphi_1),$$

i_l being the modified spherical Bessel functions,

$$\begin{aligned}i_l(z) &= z^l\left(\frac{\partial}{z\partial z}\right)^l \frac{\sinh(z)}{z} \\ &= \frac{\exp(z)}{2z}\sum_{k=0}^{l}\frac{(-1)^k(l+k)!}{k!(l-k)!(2z)^k} \\ &\quad -(-1)^l\frac{\exp(-z)}{2z}\sum_{k=0}^{l}\frac{(l+k)!}{k!(l-k)!(2z)^k}.\end{aligned}$$

This leads to the definition of the functions g_{nl} mentioned in the main text,

$$\rho_{nlm\pm} = y_{lm\pm} g_{nl}(r, \alpha, U)$$

$$g_{nl}(r, \alpha, U) = (2/\pi)^{1/2} \alpha^{n+3} U^{-3/2} \exp(-r^2/2U) \times \int_0^\infty u^{n+2} \exp(-u^2/2U - \alpha u) i_l(ru/U)\, du.$$

The preceding integral is evaluated by setting $1/2U = p$, $\alpha \pm r/U = q_\pm$,

$$D_v(p, q) = \int_0^\infty x^v \exp(-px^2 - qx)\, dx = [(-1)^v/2](\pi/p)^{1/2} \times \partial^v [\exp(q^2/4p) \operatorname{erfc}(q/2p^{1/2})]/\partial q^v.$$

This leads to the final result

$$g_{nl} = \alpha^{n+3} U^{-3/2} \exp(-r^2/2U) \times \sum_{k=0}^{l} \frac{(l+k)!}{k!(l-k)!} \left(\frac{U}{2r}\right)^{k+1} \times \{(-1)^k D_{n-k+1}(-) - (-1)^l D_{n-k+l}(+)\}; \quad (9)$$

$$D_v(\pm) = (-1)^v U^{(v+1)/2} \times \left\{ \exp[(\alpha U \pm r)^2/2U] \operatorname{erfc}\left[\frac{\alpha U \pm r}{(2U)^{1/2}}\right] \times F_v\left(\frac{\alpha U \pm r}{U^{1/2}}\right) - \left(\frac{2}{\pi}\right)^{1/2} G_v\left(\frac{\alpha U \pm r}{U^{1/2}}\right) \right\}; \quad (10)$$

$$F_{v+1}(z) = zF_v(z) + vF_{v-1}(z); \quad F_0(z) = 1; \quad F_1(z) = z, \quad (11)$$

$$G_{v+1}(z) = zG_v(z) + vG_{v-1}(z); \quad G_0(z) = 0; \quad G_1(z) = 1. \quad (12)$$

These expressions are far too complicated to solve analytically the expression $\partial\rho_{nlm\pm}/\partial r = 0$, but the positions and values of the extrema can be found with numerical methods. These calculations show that for $l = n$ the distances of the extrema from the atom center are given by

$$r_{\text{extr}}(U, \alpha) = U^{1/2} \Delta_n(z); \quad z = \alpha U^{1/2}, \quad (13)$$

$$\Delta_n(z) \simeq n/z + z \sum_{j=1}^{3} C_{nj}/(4z^j + 2n + j), \quad (14)$$

Table 5. *Coefficients C_{nj} for the evaluation of equations (13) and (14)*

n	C_{n1}	C_{n2}	C_{n3}
3	6.783597	2.775752	0.970753
4	7.881257	4.142102	0.475391
5	8.883658	5.574661	0.0

where the C_{nj} (Table 5) are determined numerically to approximate the exact solution to better than 0.3% in the range $1/4 < z < 15$. This type of calculation shows that the exponential and Gaussian deformation functions yield similar electron densities, except for small values of U.

References

Becker, P. J. & Coppens, P. (1974). *Acta Cryst.* A**30**, 129–147.

Becker, P. J. & Coppens, P. (1975). *Acta Cryst.* A**31**, 417–425.

Coppens, P. (1993). *International Tables for Crystallography*, Vol. B, pp. 10–22. Dordrecht: Kluwer.

Hester, J. R., Maslen, E. N., Spadaccini, N., Ishizawa, N. & Satow, Y. (1993). *Acta Cryst.* B**49**, 967–973.

Hirshfeld, F. L. (1977). *Isr. J. Chem.* **16**, 226–229.

Hirshfeld, F. L. (1991). *Crystallogr. Rev.* **2**, 169–204.

Holladay, A., Leung, P. & Coppens, P. (1983). *Acta Cryst.* A**39**, 377–387.

International Tables for X-ray Crystallography (1974). Vol. IV. Birmingham: Kynoch Press. (Present distributor Kluwer Academic Publishers, Dordrecht.)

Jauch, W. & Palmer, A. (1993). *Acta Cryst.* A**49**, 590–591.

Johnson, C. K. & Levy, H. A. (1974). *International Tables for X-ray Crystallography*, Vol. IV, pp. 314–319. Birmingham: Kynoch Press. (Present distributor Kluwer Academic Publishers, Dordrecht.)

Kurki-Suonio, K. (1977). *Isr. J. Chem.* **16**, 115–123.

Nowack, E., Schwarzenbach, D. & Hahn, T. (1991). *Acta Cryst.* B**47**, 650–659.

Restori, R. & Schwarzenbach, D. (1993). *Z. Naturforsch. Teil A*, **48**, 12–20.

Restori, R. & Schwarzenbach, D. (1995). *Acta Cryst.* B**51**, 261–263.

Roberto, J. B., Batterman, B. W. & Keating, D. T. (1974). *Phys. Rev. B*, **9**, 2590–2599.

Saka, T. & Kato, N. (1986). *Acta Cryst.* A**42**, 469–478.

Sakata, M. & Sato, M. (1990). *Acta Cryst.* A**46**, 263–270.

Spackman, M. A. (1986). *Acta Cryst.* A**42**, 271–281.

Stevens, E. D. & Coppens, P. (1979). *Acta Cryst.* A**35**, 536–539.

Stevens, E. D., DeLucia, M. L. & Coppens, P. (1980). *Inorg. Chem.* **19**, 813–820.

Stewart, R. F. (1976). *Acta Cryst.* A**32**, 565–574.

Teworte, R. & Bonse, U. (1984). *Phys. Rev. B*, **29**, 2102–2108.

Toriumi, K. & Saito, Y. (1983). *Adv. Inorg. Chem. Radiochem.* **27**, 27–81.

Willis, B. T. M. & Pryor, A. W. (1975). *Thermal Vibrations in Crystallography*, p. 150. Cambridge University Press.